Weak electron–phonon coupling contributing to high thermoelectric performance in n-type PbSe

Heng Wang, Yanzhong Pei[1], Aaron D. LaLonde, and G. Jeffrey Snyder[1]

Department of Materials Science, California Institute of Technology, Pasadena, CA 91125

Edited by Ali Shakouri, University of California, Santa Cruz, CA, and accepted by the Editorial Board April 13, 2012 (received for review July 14, 2011)

PbSe is a surprisingly good thermoelectric material due, in part, to its low thermal conductivity that had been overestimated in earlier measurements. The thermoelectric figure of merit, *zT*, can exceed 1 at high temperatures in both p-type and n-type PbSe, similar to that found in PbTe. While the p-type lead chalcogenides (PbSe and PbTe) benefit from the high valley degeneracy (12 or more at high temperature) of the valence band, the n-type versions are limited to a valley degeneracy of 4 in the conduction band. Yet the n-type lead chalcogenides achieve a *zT* nearly as high as the p-type lead chalcogenides. This effect can be attributed to the weaker electron–phonon coupling (lower deformation potential coefficient) in the conduction band as compared with that in the valence band, which leads to higher mobility of electrons compared to that of holes. This study of PbSe illustrates the importance of the deformation potential coefficient of the charge-carrying band as one of several key parameters to consider for band structure engineering and the search for high performance thermoelectric materials.

energy | semiconductor | quality factor

Waste heat recovery using thermoelectric power generation is attracting considerable interest from the automobile industry (1) as well as from many other areas (2). Large-scale production of bulk materials with high figure of merit, zT, defined as $zT = S^2\sigma T/(\kappa_e + \kappa_L)$ (S is the Seebeck coefficient, σ is the electric conductivity, and κ_e and κ_L are the electronic and lattice thermal conductivity, respectively), is the key to widespread adaption of thermoelectric technology. The search for good thermoelectric materials has focused on investigating semiconductors that have suitable band structures and low thermal conductivities (3, 4). As one of the first investigated material systems (5), PbTe and its alloys have been extensively studied and remain some of the best (6, 7) thermoelectric materials for applications from 500 to 900 K. Considerable effort has been made to achieve a higher zT in these alloys by reducing the lattice thermal conductivity, κ_L, by incorporation of nanometer scale inclusions (8–11). Other strategies approach the challenge of increasing zT from different angles, such as band structure distortion by Tl doping (12), and more recently, increasing band degeneracy by converging two different valence bands in p-type PbTe (13).

It can be shown that the material parameter called the thermoelectric quality factor, B,

$$B = \left(\frac{k_B}{e}\right)^2 \frac{2e(k_B T)^{3/2}}{(2\pi)^{3/2}\hbar^3} \frac{N_V \mu_0 m_b^{*3/2}}{\kappa_L} T \qquad [1]$$

determines the optimized figure of merit (14–16) (N_V is the band degeneracy, m_b^* is the density of states effective mass of a single band, μ_0 is the mobility at nondegenerate limit, and κ_L is the lattice thermal conductivity). This expression is derived for semiconductors with single band transport behavior where the carrier concentration can be optimized to achieve maximum zT. For good thermoelectric semiconductors the dominant scattering mechanism at high temperatures, where zT peaks, is typically due to acoustic phonons. The deformation potential theory of Bardeen and Shockley (17) enables the nondegenerate mobility, μ_0, in B to be replaced with parameters more descriptive of the band structure, namely the effective mass and deformation potential coefficient, Ξ, of the conducting band. This gives the resulting expression when multivalley conduction is considered (18):

$$\mu_0 = \frac{2^{3/2}\pi^{1/2}\hbar^4 e C_l}{3m_I^*(m_b^* k_B T)^{3/2}\Xi^2}, \qquad [2]$$

where m_I^* is the inertial effective mass and C_l is a combination of elastic constants. The deformation potential coefficient describes the change in energy of the electronic band with elastic deformation and thus describes the interaction, or coupling, between electrons and phonons.

Including this relationship in the expression for B reveals

$$B = T\frac{2k_B^2\hbar}{3\pi}\frac{C_l N_V}{m_I^*\Xi^2\kappa_L}. \qquad [3]$$

Because κ_L is generally independent of electronic band structure* (19), this relation for B suggests that Ξ is an important factor determining the maximum performance of a thermoelectric material.

The high thermoelectric performance of p-type PbSe, a lower cost analog of PbTe, has been a relatively recent discovery (20–22). Originally, PbSe was thought to be significantly inferior to PbTe because of higher thermal conductivity and lower band gap (22). This turns out not to be the case at high temperatures where zT is greatest. The lattice thermal conductivity of PbSe is nearly as low as PbTe because of the larger (21) Grüneisen parameter of PbSe relative to PbTe while the band gap of PbSe increases rapidly with temperature, actually exceeding that of PbTe above 500 K (23, 24). Like with PbTe, the zT for PbSe can be greater than 1 with dense samples, optimal doping, and utilizing the thermal diffusivity technique for thermal conductivity measurements. In this study, we have measured a peak zT for Br-doped PbSe to be 1.1 ± 0.1 at 850 K in five different samples, using different measurement techniques in different institutions on the same sample (see Fig. 1 and *SI Material* for comparison of each property and zT for Br-doped samples measured at Caltech,

Author contributions: H.W., Y.P., and G.J.S. designed research; H.W. performed research; A.D.L. contributed new reagents/analytic tools; H.W. analyzed data; H.W., Y.P., and G.J.S. discussed results; and H.W., Y.P., and G.J.S. wrote the paper.

The authors declare no conflict of interest.

This article is a PNAS Direct Submission. A.S. is a guest editor invited by the Editorial Board.

*When κ_L is dominated by Umklapp scattering, typically the most important phonon scattering process for thermoelectrics above room temperature, it can be related to other physical properties as $\kappa_L \propto \frac{V^{1/3}C^{\infty}}{T\gamma^2\sqrt{d}}$. In the case for glass-like phonon thermal conductivity, κ_L is related to these properties as $\kappa_L \propto \frac{\sqrt{C}}{V^{2/3}\sqrt{d}}$, where C is a combination of elastic moduli, d is the density, V is the volume per atom and γ the Grüneisen parameter (see ref. 19). The parameters characterizing the electronic band structure, such as deformation potential, are not seen in these relations

[1]To whom correspondence may be addressed. Email: jsnyder@caltech.edu or yanzhong@caltech.edu.

This article contains supporting information online at www.pnas.org/lookup/suppl/doi:10.1073/pnas.1111419109/-/DCSupplemental.

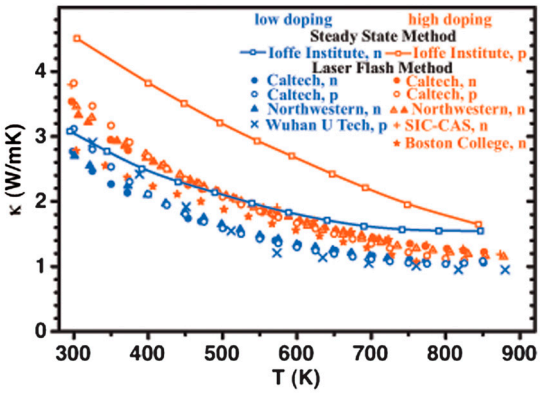

Fig. 1. A comparison of thermal conductivity of PbSe measured using the steady-state method and the laser flash method. Data are shown in two different groups (details shown in *SI Material*) according to the carrier density. All the laser flash measurements show similar behavior despite the differences in composition, while the steady-state method gives higher thermal conductivities.

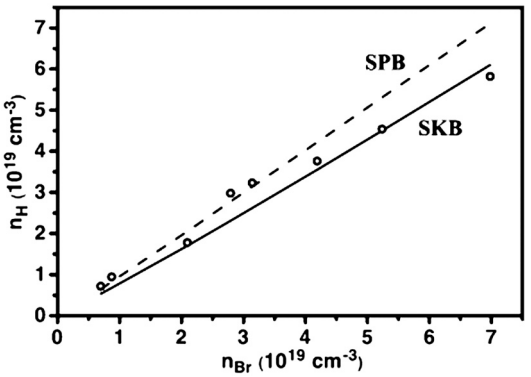

Fig. 2. The measured Hall carrier density as a function of Br concentration. The observed value matches reasonably well with expected value using the single Kane band model (SKB) or single parabolic band model (SPB).

Shanghai Institute of Ceramics–Chinese Academy of Sciences, and Jet Propulsion Laboratory).

Early measurement on optimally doped PbTe and PbSe had overestimated the thermal conductivity, which has led to an underestimate (7) of zT. This overestimation of thermal conductivity can be traced to the unavailability of data (25) or the technique for high temperature thermal conductivity. Today the most used technique for high temperature thermal conductivity is the flash diffusivity method as opposed to the steady-state method because of inaccuracies resulting from radiation losses during measurement (26). Our thermal conductivity measurements on PbSe are consistent with those of other laboratories using the same diffusivity technique (some reported subsequent to the original submission of this manuscript). The thermal conductivity measured by the steady-state method (22) is significantly higher than that measured by five independent groups using the diffusivity technique (Fig. 1).

Additionally, high zT in p-type PbSe is attributed to the high band degeneracy ($N_V \geq 12$) at high temperatures (13, 21). Conversely, the conduction band for PbSe has a much lower band degeneracy of 4. With these attributes in mind, n-type PbSe should not be expected to have high zT; nevertheless, with optimized carrier density, zT is found to be as high as approximately 1.2 at 850 K, as shown below. The explanation for the surprisingly large zT is a smaller deformation potential coefficient of the conduction band compared to the valence band, as evidenced by high carrier mobility resulting from weak scattering.

N-type PbSe is formed by substitution of Se^{2-} with a halogen, such as Br^{-}, with one conducting electron produced for each substituted atom. A slight amount of excess Pb is commonly used (25, 27) to minimize compensating metal vacancies that lead to p-type conduction as well as to improve the mechanical strength. Br is chosen in this study because it is closest in atomic size and electronic structure to Se and thus is expected to have minimal effect on the carrier mobility.

The Hall carrier density ($n_H = 1/eR_H$, R_H is the measured Hall coefficient) can be tuned from 7×10^{18} to 5×10^{19} cm^{-3} by controlling the dopant concentration. The samples are identified with their Hall carrier density at 300 K for the following discussion while their nominal compositions are given in *SI Material*.

The measured values of n_H are in good agreement with expected value based on Br content (Fig. 2). Exactly one electron in the conduction band per Br atom is expected for $PbSe_{1-x}Br_x$ based on the simple valence principle, which provides a good model for heavily doped thermoelectric semiconductors (28). Earlier results on Cl doped PbSe appear to follow this valence principle (22), while more recent results on Cl doped PbSe show far fewer carriers than expected. The fewer than expected carriers may indicate the presence of other bulk or surface defects that lead to the reduced mobility of these samples (29).

PbSe is a small band gap semiconductor in which the direct band gap forms between bands with small band mass (30). The band extrema is located at the L point of the Brillouin zone and has four equivalent ellipsoid pockets (24) ($N_V = 4$) that dominate the transport properties for n-type PbSe. As with all lead chalcogenides, the conduction band (and the light valence band) have been shown to be nonparabolic (7, 23, 31–33), with transport properties that can be well characterized by the single Kane band (SKB) model (24). It is confirmed here that the SKB model quantitatively explains the observed electronic transport properties throughout the temperature and doping range discussed in this paper (*SI Material*).

Both the Seebeck coefficient and resistivity increase with increasing temperature for the majority of the samples in this study, as shown in Fig. 3 *A* and *B*, respectively. These trends are consistent with degenerate semiconducting behavior.

The total thermal conductivity (Fig. 3*C*) decreases with temperature, reducing to 1.0–1.4 W/mK at 850 K, depending on the doping level. The lattice thermal conductivity, κ_L, is calculated by subtracting the electronic contribution ($\kappa_e = LT/\rho$) from the measured total thermal conductivity, where L is calculated using the SKB model. The κ_L for several optimally doped samples, as well as the averaged value (dashed line), are shown in *SI Material* and indicate a κ_L of approximately 0.8 W/mK at 850 K, which is consistent with the previously reported (21) value for κ_L of p-type PbSe (approximately 0.6 W/mK at 850 K)

The zT values as a function of temperature are shown in Fig. 4. The optimal doping level is found to be around 3×10^{19} cm^{-3}, achieving zT as high as 1.2 at 850 K. The zT value of $1.0 \sim 1.2$ was obtained in multiple samples with room temperature n_H between 2.9 and 3.4×10^{19} cm^{-3} and whose transport properties were measured both perpendicular and parallel to the hot press direction (*SI Material*).

It may be surprising that $zT > 1$ can be achieved in properly doped n-type PbSe where a single band with a relatively small $N_V = 4$ is responsible for the electronic transport properties. In comparison, the light valence band of p-type PbSe with same m_b^* and N_V as the conduction band has a much lower zT (*SI Material*). Properly doped p-type PbSe achieves high zT at high temperatures due to the influence of the heavy valence band, which produces an extraordinarily large number of valleys ($N_V \geq 12$) (13, 21). Thus, high zT in n-type PbTe suggests an advantage in the character of the conduction band that compensates for the relatively low number of degenerate valleys. The accuracy of the SKB model in characterizing carrier transport in the light bands at the L point, in combination with the fact that

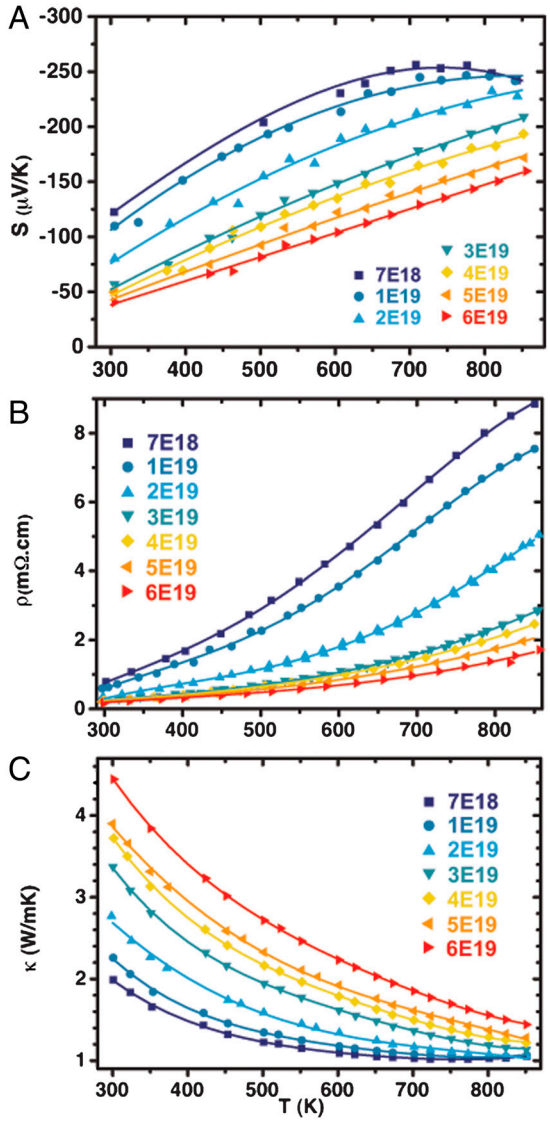

Fig. 3. Thermoelectric transport properties of Br-doped PbSe as function of temperature. (*A*) Seebeck coefficient, (*B*) resistivity, and (*C*) thermal conductivity.

the effective mass and elastic properties (i.e., C_l) of the n-type and p-type PbSe are found to be the same, allow for the compensating effect in the n-type material to be traced to the deformation potential coefficient (Ξ), as discussed below.

Fig. 5*A* shows the Seebeck coefficient versus Hall carrier density at 300 K for both n- and p-type samples. The agreement of the calculated curve for both materials indicates that the density of states effective mass, $m^* = N_V{}^{2/3} m_b{}^*$, is the same ($m^* = 0.27\, m_e$) for both the conduction band and the light valence band. In addition, the speed of sound was measured and found to be comparable ($v_l \approx 3{,}200$ m/s, $v_t \approx 1{,}700$ m/s) for both p- and n-type PbSe. By these consistencies, it is implied that the parameter C_l, determined by the elastic moduli, remains unchanged for both n- and p-type samples.

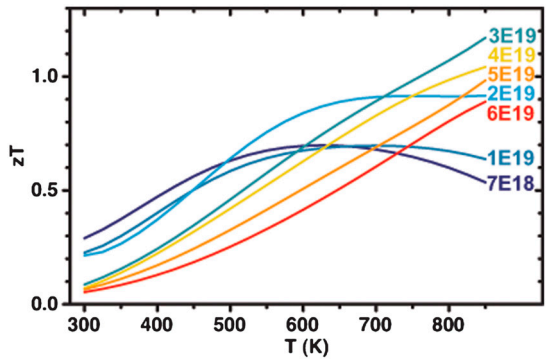

Fig. 4. *zT* as function of temperature for Br-doped PbSe.

Fig. 5*B* shows the Hall mobility (μ_H) of n- and p-type samples at 300 K as well as data reported by Smirnov (34), Allgaier (35), and Androulakis (29). The p-type samples are selected such that the carrier density is relatively low and thus the influence from the heavy band at this temperature is negligible. It is clearly seen that the mobility of the n-type material is much higher than that of the p-type material over the entire carrier density range [there are previous studies supporting this result (34, 36, 37), while there are also other reports suggesting that the mobility is similar between n- and p-type PbSe at room temperature (35, 38)]. Furthermore, the SKB model provides excellent prediction of μ_H vs. n_H at 300 K for both n- and p-type materials at high doping levels where acoustic phonon scattering is the dominant mechanism. The curves to model the mobility data for each material can be obtained by using different deformation potential coefficient values (in absolute value), while all other model parameters are the same: for n-type samples, the parameter is Ξ = 25 eV, while for p-type samples, Ξ = 35 eV. The deformation potential coefficient represents the degree to which the charge carriers interact with phonons in the material. Therefore, the lower Ξ value in the n-type material reveals that the carriers are less scattered by acoustic phonons in the conduction band compared with those in the valence band.

The result that Ξ is approximately 10 eV smaller in the conduction band than in the light valence band is supported by both calculations and experimental characterization of the optical deformation potential, D_{iso}, of both PbSe and PbTe. By definition, D_{iso} is calculated by subtracting the isotropic deformation

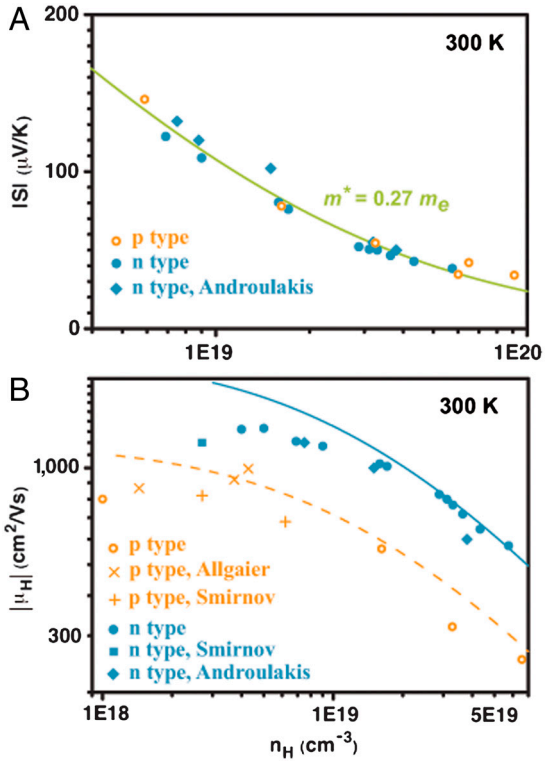

Fig. 5. Thermoelectric properties of n-type and p-type PbSe. (*A*) Seebeck coefficient and (*B*) Hall mobility as function of Hall carrier density at 300 K. All curves are calculated from SKB model.

potential, which is related to Ξ (39), of the valence band from that of the conduction band, where both values are negative for lead chalcogenides. Zasavitskii (40) determined $D_{iso} = 14$ eV at 295 K for PbSe in quantum well structures from photoluminescence and X-ray diffraction data. Ferreira (41) calculated D_{iso} to be approximately 10 eV for PbTe using the Augmented-Plane-Wave method. These values are in reasonable agreement with the D_{iso} estimated from the elastic moduli (42) and the experimental change in band gap due to pressure (24) [approximately 13 eV for PbSe, approximately 10 eV for PbTe (41)] as well as thermal expansion and temperature dependence of the energy gap (24) [approximately 21 eV for PbSe, approximately 15 eV for PbTe (41)] using the relationship given by Ferreira (41).

The temperature dependent Seebeck coefficient and resistivity of both n- and p-type PbSe are compared with the SKB model results and shown in Fig. 6 *A* and *B*, respectively. The two samples shown have approximately the same carrier density ($n_{H,300\,K} \sim 3 \times 10^{19}$ cm^{-3}). Using parameters determined in this work, the SKB model successfully predicts both the Seebeck coefficient and resistivity for n-type PbSe up to 850 K. The SKB model is poor for p-type PbSe, especially at high temperatures, due to the transport behavior resulting from two contributing bands. Most importantly, it is clearly seen that at lower temperatures, where the light valence band dominates the transport properties of p-type PbSe (Fig. 6*B*), n-type PbSe shows much weaker carrier scattering (due to smaller Ξ) than p-type material, resulting in a lower resistivity, and ultimately high zT.

In the single Kane band model, the same quality factor B defined by Eq. **3** is found to characterize the suitability of the band structure through the expression of zT:

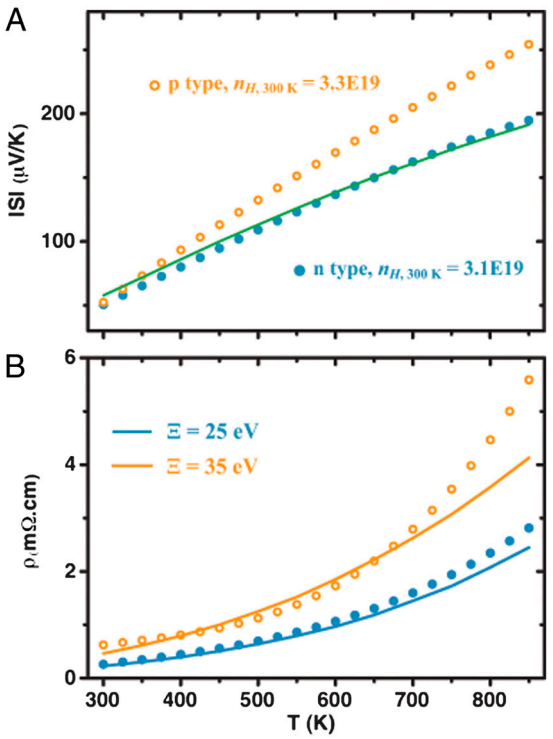

Fig. 6. Thermoelectric properties (*A*) Seebeck coefficient and (*B*) resistivity for n-type and p-type PbSe having similar carrier density. All curves are calculated from SKB model (note that the calculated Seebeck coefficient for the n- and p-type is the same and does not depend on Ξ) showing that while the n-type data fits the SKB model at all temperatures well, the p-type shows deviations at higher temperature due to two-band behavior.

$$zT = \left[\frac{{}^1F^1_{-2}}{{}^0F^1_{-2}} - \xi\right]^2 \Big/ \left\{\left[\frac{{}^2F^1_{-2}}{{}^0F^1_{-2}} - \left(\frac{{}^1F^1_{-2}}{{}^0F^1_{-2}}\right)^2\right] + B^{-1}({}^3{}^0F^1_{-2})^{-1}\right\}. \quad [4]$$

The ξ and ${}^nF^m_l$ (see *SI Material* for definition) dependent terms can be optimized via carrier density tuning. Subsequently, the maximum zT one could achieve for the optimized carrier density is determined by the quality factor B. In p-type PbSe the effective band degeneracy, N_V, is large because of the convergence of two different valence bands, which leads to a large B and high zT. In n-type PbSe, although N_V is smaller, high zT is achieved as a result of comparable quality factor, B, which stems from a smaller Ξ.

Ξ for a few semiconductor systems are found in the range of 5 to 35 eV (*SI Material*). Given a certain material system, the maximum zT achieved by carrier density tuning would be further increased if the deformation potential of bands participating in carrier transport could be engineered. The latter has been shown possible at least in low dimensional systems: Murphy-Armando and Fahy (43) found that the deformation potential of Γ band of n-type Ge film is decreased with strain. Also, in Si thin films embedded between hard layers of diamond (44), the mobility is found increased due to suppressed deformation potential electron–phonon scattering.

Since the original submission of this manuscript there have been reports on transport properties in n-type PbSe doped with group III elements (45) and chlorine (29), as well as nanostructured (46) $PbSe_{1-x}S_x$. Our discussion here involves complementary phenomena that should have some applicability to these results.

In summary, n-type PbSe doped with Br achieves zT values exceeding 1 at 850 K, similar to that found in p-type PbSe, making PbSe a competitive and less expensive alternative to PbTe for both types. In p-type PbSe, high zT is achieved due to the convergence of the light and heavy valence bands, acting to effectively increase band degeneracy. In n-type PbSe, with relatively low band degeneracy, high zT is achieved as a result of a low deformation potential coefficient characterizing weak scattering of the charge carriers in the conduction band. This study demonstrates the importance of the deformation potential coefficient in selecting and engineering optimum band structures for thermoelectrics.

This paper highlights a discrepancy between thermal conductivity data obtained via commonly accepted laser flash method compared to the less commonly used steady-state method such as that performed by the Ioffe Institute. Because the Ioffe technique includes a radiation shield and finds no significant error resulting from radiation losses during measurement, there is no reason to believe the Ioffe data are less reliable. Thus, it will be important to the field to organize a comprehensive comparison between the two methods.

Materials and Methods

Polycrystalline samples of $Pb_{1.002}Se_{1-x}Br_x$ with x changing from 0.04% to 0.4% were prepared using a melt alloying and hot pressing technique. Pure elements and $PbBr_2$ (Pb, 99.999%; Se, 99.999%; $PbBr_2$ 99.999%, ultra dry) were weighed out according to each composition and loaded into quartz ampoules, which were then evacuated and sealed. The sealed ampoules were slowly heated up to 1,400 K and kept for 12 h followed by a water quench. The ingots obtained were further annealed at 950 K for 72 h before being crushed and ground into fine powders. The powders were then hot pressed (47) at 873 K under 1 atm argon with 40 MPa pressure for 20 min, followed by another 60 min of annealing at 873 K without pressure. A typical disk shaped sample obtained is 12 mm in diameter, approximately 1 mm in thickness, with density no less than 98% of theoretical density (8.27 g/cm^3). Samples were single phase according to XRD results on the hot pressed disks. Analysis by a scanning Seebeck probe showed homogeneous Seebeck coefficient with standard deviation of 3.7 μV/K (approximately 5% in Seebeck coefficient).

The in-plane resistivities and Hall coefficients (R_H) were measured using the Van der Pauw method in a magnetic field up to ± 2 T. The free surface of the sample was coated with insulating BN, which successfully prevented sample degradation at high temperature in vacuum. The Seebeck coefficients were obtained along the cross-plane direction by measuring the thermoelectric voltages as well as temperatures (48). The cross-plane thermal conductivities were obtained from $\kappa = dD_T C_p$, with the thermal diffusivity D_T measured by the laser flash method (Netzsch LFA 457), where d is the geometric density. The heat capacity C_p was determined using the equation C_p/k_B atom$^{-1} = 3.07 + 4.7 \times 10^{-4}$ (T/K-300) based on experimental results (49) and is believed to be accurate for lead chalcogenides (7, 13, 21, 50, 51).

All the measurements were carried out under vacuum, and data were collected during both heating and cooling with both datasets shown. As seen in the figures, no hysteresis was observed. In addition, the temperature dependent resistivities were retested after the other high temperature measurements were done, and no appreciable change was found. The uncertainty of each measurement is estimated to be approximately 5%, which combined leads to approximately 20% uncertainty for zT. More details about the measurement uncertainty are discussed in the supplementary material.

ACKNOWLEDGMENTS. The authors thank Xun Shi and Lidong Chen at Shanghai Institute of Ceramics–Chinese Academy of Science and Alexandra Zevalkink at Jet Propulsion Laboratory for confirming measurements, and Defense Advanced Research Planning Agency's Nano-Structured Materials for Power program and National Aeronautics and Space Administration–Jet Propulsion Laboratory for financial support.

1. Bell LE (2008) Cooling, heating, generating power, and recovering waste heat with thermoelectric systems. *Science* 321:1457–1461.
2. Kajikawa T (2006) *CRC Thermoelectric Handbook*, ed DM Rowe (CRC Press, Boca Raton, FL), pp 50-1–50-26.
3. Snyder GJ, Toberer ES (2008) Complex thermoelectric materials. *Nat Mater* 7:105–114.
4. Minnich AJ, Dresselhaus MS, Ren ZF, Chen G (2009) Bulk nanostructured thermoelectric materials: Current research and future prospects. *Energy Environ Sci* 2:466–479.
5. Wood C (1988) Materials for thermoelectric energy-conversion. *Rep Prog Phys* 51:459–539.
6. Pei Y, LaLonde A, Iwanaga S, Snyder GJ (2011) High thermoelectric figure of merit in heavy hole dominated PbTe. *Energy Environ Sci* 4:2085–2089.
7. LaLonde AD, Pei Y, Snyder GJ (2011) Reevaluation of PbTe1-xIx as high performance n-type thermoelectric material. *Energy Environ Sci* 4:2090–2096.
8. Pei Y, Lensch-Falk J, Toberer ES, Medlin DL, Snyder GJ (2011) High thermoelectric performance in PbTe due to large nanoscale Ag2Te precipitates and La doping. *Adv Funct Mater* 21:241–249.
9. Pei Y, May AF, Snyder GJ (2011) Self-tuning the carrier concentration of PbTe/Ag2Te composites with excess Ag for high thermoelectric performance. *Adv Energy Mater* 1:291–296.
10. He JQ, Girard SN, Kanatzidis MG, Dravid VP (2010) Microstructure-lattice thermal conductivity correlation in nanostructured PbTe07S0.3 Thermoelectric Materials. *Adv Funct Mater* 20:764–772.
11. Poudeu PFR, et al. (2006) High thermoelectric figure of merit and nanostructuring in bulk P-Type Na1-XPbmSbyTem+2. *Angew Chem Int Ed Engl* 45:3835–3839.
12. Heremans JP, et al. (2008) Enhancement of thermoelectric efficiency in PbTe by distortion of the electronic density of states. *Science* 321:554–557.
13. Pei Y, et al. (2011) Convergence of electronic bands for high performance bulk thermoelectrics. *Nature* 473:66–69.
14. Goldsmid HJ (1964) *Thermoelectric Refrigeration* (Temple Press Books LTD, London).
15. Mahan GD (1998) *Solid State Physics Vol 51: Solid State Physics—Advances in Research and Applications* (Academic, New York), pp 81–157.
16. Chasmar RP, Stratton R (1959) The thermoelectric figure of merit and its relation to thermoelectric generators. *J Electron Control* 7:52–72.
17. Bardeen J, Shockley W (1950) Deformation potentials and mobilities in non-polar crystals. *Phys Rev* 80:72–80.
18. Herring C, Vogt E (1956) Transport and deformation potential theory for many-valley semiconductors with anisotropic scattering. *Phys Rev* 101:944–961.
19. Toberer ES, Zevalkink A, Snyder GJ (2011) Phonon engineering through crystal chemistry. *J Mater Chem* 21:15843–15852.
20. Parker D, Singh DJ (2010) High-temperature thermoelectric performance of heavily doped PbSe. *Phys Rev B* 82:035204.
21. Wang H, Pei Y, Lalonde AD, Snyder GJ (2011) Heavily doped p-type PbSe with high thermoelectric performance: An alternative for PbTe. *Adv Mater* 23:1366–1370.
22. Alekseeva GT, Gurieva EA, Konstantinov PP, Prokofeva LV, Fedorov MI (1996) Thermoelectric figure of merit of hetero- and isovalently doped PbSe. *Semiconductors* 30:1125–1127.
23. Veis AN, Kuteinikov RF, Kumzerov SA, Ukhanov YI (1976) Investigation of valence band-structure of lead selenide by optical methods. *Sov Phys Semiconductors* 10:1320–1321.
24. Ravich YI, Efimova BA, Smirnov IA (1970) *Semiconducting Lead Chalcogenides* (Plenum Press, New York), pp 85–216.
25. Fritts RW (1960) *Thermoelectric Materials and Devices*, eds IB Cadoff and E Miller (Reinhold Pub Corp, New York), pp 143–162.
26. Parker WJ, Jenkins RJ, Abbott GL, Butler CP (1961) Flash method of determining thermal diffusivity, heat capacity, and thermal conductivity. *J Appl Phys* 32:1679.
27. Kovalchik TL, Maslakovets IP (1956) Effect of impurities on the electrical properties of lead telluride. *Sov Phys Tech Phys* 1:2337–2349.
28. Toberer ES, May AF, Snyder GJ (2010) Zintl chemistry for designing high efficiency thermoelectric materials. *Chem Mat* 22:624–634.
29. Androulakis J, et al. (2011) High-temperature charge and thermal transport properties of the n-type thermoelectric material PbSe. *Phys Rev B* 84:155207.
30. Lach-hab M, Papaconstantopoulos DA, Mehl MJ (2002) Electronic structure calculations of lead chalcogenides PbS, PbSe, PbTe. *J Phys Chem Solids* 63:833–841.
31. Stavitskaya TS, Prokofeva IV, Ravich YI, Efimova BA (1968) Influence of conduction-band nonparabolicity on transport coefficients of PbTe in temperature range 100–1000 degrees K. *Sov Phys Semiconductors* 1:952–957.
32. Dubrovskaya IN, Efimova BA, Nensberg ED (1968) Investigation of nonparabolicity of conduction bands of PbSe and PbS. *Sov Phys Semiconductors* 2:436–440.
33. Chernik IA, Kaidanov VI, Ishutinov EP (1961) Dispersion relation for conduction band of lead selenide. *Sov Phys Semiconductors* 2:825–829.
34. Smirnov IA, Moizhes BY, Nensberg ED (1961) The effective carrier mass in lead selenide. *Sov Phys Solid State* 2:1793–1804.
35. Allgaier RS, Scanlon WW (1958) Mobility of electrons and holes in PbS, PbSe, and PbTe between room temperature and 4.2-degrees-K. *Phys Rev* 111:1029–1037.
36. Ravich YI (2003) *Lead Chalcogenides Physics and Applications Vol 18 Optoelectronic Properties of Semiconductors and Superlattices*, ed D Khokhlov (Taylor & Francis, New York).
37. Vinogradova MN, Gunko TS, Ukhanov YI, Tselishc NS, Shershne LM (1971) Investigation of reflection of infrared radiation from heavily doped samples of n-type and p-type PbSe. *Sov Phys Semiconductors* 4:1686–1690.
38. Schlichting U, Gobrecht KH (1973) Mobility of free carriers in PbSe crystals. *J Phys Chem Solids* 34:753–758.
39. Ravich YI, Efimova BA, Tamarchenko VI (1971) Scattering of current carriers and transport phenomena in lead chalcogenides. 2. Experiment. *Phys Status Solidi B Basic Res* 43:453–469.
40. Zasavitskii II, Silva E, Abramof E, McCann PJ (2004) Optical deformation potentials for PbSe and PbTe. *Phys Rev B* 70:115302.
41. Ferreira LG (1965) Deformation potentials of lead telluride. *Phys Rev* 137:1601–1609.
42. Lippmann G, Kastner P, Wanninge W (1971) Elastic constants of PbSe. *Phys Status Solidi A Appl Res* 6:K159–K161.
43. Murphy-Armando F, Fahy S (2011) Giant enhancement of n-type carrier mobility in highly strained germanium nanostructures. *J Appl Phys* 109:113703.
44. Nika DL, Pokatilov EP, Balandin AA (2008) Phonon-engineered mobility enhancement in the acoustically mismatched silicon/diamond transistor channels. *Appl Phys Lett* 93:173111.
45. Androulakis J, Lee Y, Todorov I, Chung DY, Kanatzidis M (2011) High-temperature thermoelectric properties of n-type PbSe doped with Ga, In, and Pb. *Phys Rev B* 83:195209.
46. Androulakis J, et al. (2011) Thermoelectrics from abundant chemical elements: High-performance nanostructured PbSe-PbS. *J Am Chem Soc* 133:10920–10927.
47. LaLonde AD, Ikeda T, Snyder GJ (2011) Rapid consolidation of powdered materials by induction hot pressing. *Rev Sci Instrum* 82:025104.
48. Iwanaga S, Toberer ES, Lalonde A, Snyder GJ (2011) A high temperature apparatus for measurement of the Seebeck Coefficient. *Rev Sci Instrum* 82:063905.
49. Blachnik R, Igel R (1974) Thermodynamic properties of IV-VI compounds lead chalcogenides. *Z Naturforsch B* 29:625–629.
50. Yamaguchi K, Kameda K, Takeda Y, Itagaki K (1994) Measurements of high-temperature heat-content of the II-VI and IV-VI (II-Zn, Cd IV-Sn, Pb VI-Se, Te) compounds. *Mater Trans JIM* 35:118–124.
51. Pashinkin AS, Mikhailova MS, Malkova AS, Fedorov VA (2009) Heat capacity and thermodynamic properties of lead selenide and lead telluride. *Inorg Mater* 45:1226–1229.